Signal transduction pathway of TonB-dependent transporters

Andrew D. Ferguson*†, Carlos A. Amezcua*, Najeeb M. Halabi‡, Yogarany Chelliah§, Michael K. Rosen*‡§, Rama Ranganathan‡§, and Johann Deisenhofer*§¶

Departments of *Biochemistry and ‡Pharmacology and §Howard Hughes Medical Institute, University of Texas Southwestern Medical Center, Dallas, TX 75390; and †Merck Research Laboratories, Rahway, NJ 07065

Contributed by Johann Deisenhofer, November 8, 2006 (sent for review March 29, 2006)

Transcription of the ferric citrate import system is regulated by ferric citrate binding to the outer membrane transporter FecA. A signal indicating transporter occupancy is relayed across the outer membrane to energy-transducing and regulatory proteins embedded in the cytoplasmic membrane. Because transcriptional activation is not coupled to ferric citrate import, an allosteric mechanism underlies this complex signaling mechanism. Using evolution-based statistical analysis we have identified a sparse but structurally connected network of residues that links distant functional sites in FecA. Functional analyses of these positions confirm their involvement in the mechanism that regulates transcriptional activation in response to ferric citrate binding at the cell surface. This mechanism appears to be conserved and provides the structural basis for the allosteric signaling of TonB-dependent transporters.

bacterial iron transport | NMR | signaling domain | statistical coupling analysis

Although iron is required by all living cells, acquiring this metal is difficult because it is essentially insoluble under physiological conditions. To solve this problem, bacteria secrete iron chelators (siderophores) that avidly scavenge ferric ions and actively pump these molecules back into the cell using TonB-dependent transporters (1). A complex of three proteins, TonB, ExbB, and ExbD, couple a proton gradient maintained across the cytoplasmic membrane to energize siderophore import across the outer membrane by these transporters. Although the precise mechanism by which this complex couples electrochemical potential to siderophore import remains unclear, an essential step is the direct interaction between the periplasmic domain of TonB and the conserved N-terminal signature sequence (termed the TonB-box) of the transporter [Fig. 1*A* and supporting information (SI) Fig. 5]. Members of the diverse family of TonB-dependent transporters include those for ferric citrate (FecA), ferrichrome (FhuA), ferric enterobactin (FepA), and other organometallic compounds such as vitamin B_{12} (BtuB).

The siderophore-mediated interaction between TonB and TonB-dependent transporters presents a well defined case study of long-range (allosteric) communication between distant functional sites. The binding of TonB to the TonB-box at the periplasmic surface is somehow dependent on siderophore binding at the extracellular surface, and this event is followed by yet unclear conformational changes in the transporter that drive siderophore import. How does siderophore binding in the extracellular pocket of the transporter regulate binding activities at the periplasmic surface? Crystallographic studies reveal that these TonB-dependent transporters comprise a 22-stranded β-barrel with an internal "plug" that is tightly lodged inside the barrel (1). As might be expected, ferric citrate binding to FecA causes several local conformational changes: (*i*) the seventh and eighth extracellular loops of the barrel close over the bound siderophore, and (*ii*) several apical loops of the plug are translated toward the ferric citrate molecule (Fig. 1*B*) (2). In addition, ferric citrate binding also triggers distant conformational changes in the periplasmic pocket of FecA as the so-called switch helix unwinds and large changes occur in the relative position and conformation of the TonB-box (Fig. 1*C*) (2, 3). Similar distant structural changes are observed upon ligand binding to other TonB-dependent transporters, suggesting that these allosteric effects are fundamentally conserved properties (1). However, although some intramolecular energy transmission mechanism must exist, no structural changes are observed that link these two regions of conformational change. This mechanism may involve propagated conformational changes that occur below the resolution of the crystal structures or may involve dynamic modes that are fundamentally not revealed by crystal structures; regardless, the allosteric mechanism underlying energetic communication by TonB-dependent transporters remained unresolved.

In addition to transport, FecA performs another important function: ligand-dependent transcriptional regulation of the ferric citrate import operon (SI Fig. 5). This activity is mediated by a unique periplasmic segment termed the signaling domain (residues 1–79), whose activity also depends on TonB binding to FecA. The signaling domain relays transporter occupancy to the regulatory protein FecR in the cytoplasmic membrane (4, 5), which then releases the σ factor FecI into the cytoplasm (4, 6–8). FecI promotes binding of RNA polymerase to the promoter upstream of the ferric citrate import operon, thereby initiating transcription (9, 10). Although transport and signaling are ferric citrate- and TonB-dependent processes, these functions are ultimately separable because removing the signaling domain abolishes ferric citrate-mediated transcriptional activation, whereas ferric citrate import remains unaffected (11, 12).

In this work we take a two-part approach to understand the TonB-dependent allosteric processes in FecA. First, using NMR spectroscopy we determined the structure of the signaling domain and constructed a complete 3D model of FecA. We then applied an evolution-based statistical method to define the ferric citrate-mediated signal transduction network within FecA. We validated these predictions by functional analyses and propose a siderophore-mediated signal transduction pathway that is conserved among TonB-dependent transporters.

Results

Signaling Domain Structure. The solution NMR structures of the signaling domains of FecA and PupA (a functionally related

Author contributions: A.D.F., M.K.R., and R.R. designed research; A.D.F., C.A.A., N.M.H., and Y.C. performed research; C.A.A. contributed new reagents/analytic tools; A.D.F., C.A.A., N.M.H., M.K.R., and R.R. analyzed data; and A.D.F., R.R., and J.D. wrote the paper.

The authors declare no conflict of interest.

Freely available online through the PNAS open access option.

Abbreviation: SCA, statistical coupling analysis.

Data deposition: The atomic coordinates for the signaling domains of FecA and PupA have been deposited in the Protein Data Bank, www.pdb.org (PDB ID codes 1ZZV and 2A02).

¶To whom correspondence should be addressed. E-mail: johann.deisenhofer@utsouthwestern.edu.

This article contains supporting information online at www.pnas.org/cgi/content/full/0609887104/DC1.

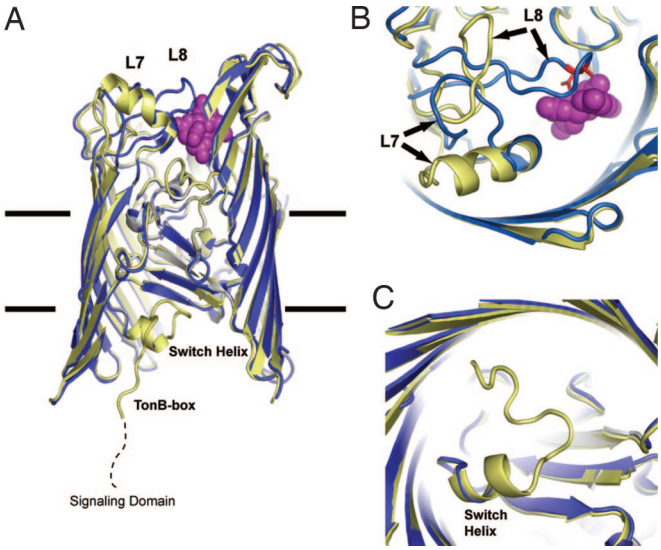

Fig. 1. Ferric citrate-mediated conformational changes in FecA. (*A*) Superposition of FecA without (yellow) and with (blue) ferric citrate (magenta). The front of the barrel has been removed for clarity. The signaling domain is attached to the plug by a flexible linker (dashed line). Binding ferric citrate causes conformational changes in the barrel and the translation of several apical loops of the plug toward the ferric citrate molecule. (*B*) Close-up of the extracellular pocket as seen from the solvent. Ferric citrate binding causes conformational changes in L7 and L8 and the closing of the extracellular pocket. (*C*) Close-up of the periplasmic pocket as seen from the periplasm. Binding ferric citrate induces the unwinding of the switch helix and changes in the relative position of the TonB-box. All figures were prepared with PyMOL (41).

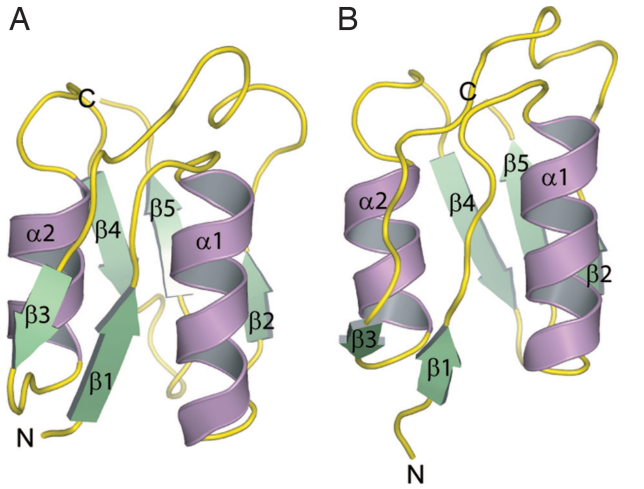

Fig. 2. NMR structure of the signaling domain. The ribbon diagram shows the conformer closest to the mean from the ensemble of FecA (*A*) and PupA (*B*) with purple α-helices, green β-strands, and yellow loops. Residues 75–80 of FecA and residues 76–81 of PupA are disordered and are not shown.

TonB-dependent transporter from *Pseudomonas putida*) were determined by standard double and triple resonance techniques (SI Table 2). A combination of proton–proton distances, dihedral angles, hydrogen bonds, and residual dipolar couplings were used in the structure calculations (SI Fig. 6). The signaling domain is ≈25 Å high and ≈21 Å wide and presents a novel mixed α/β-fold comprised of two α-helices and two antiparallel β-sheets that alternate around an internal pseudotwofold symmetry axis (Fig. 2). The protein sequences of the signaling domains of FecA and PupA are 25% identical; the structures are similar with an overall rmsd of 1.8 Å. Because the conserved residues form the hydrophobic core of the signaling domain (SI Fig. 7), this fold is most likely conserved among functionally related TonB-dependent transporters. The NMR structure of a longer construct of the signaling domain of FecA (residues 1–95, which includes the TonB-box) was recently reported (13). Although the structures are largely similar (overall rmsd of 2.3 Å), significant differences are found at the N terminus of the signaling domain. A detailed discussion of these differences can be found in the legend of SI Fig. 8.

The C terminus of the signaling domain consists mainly of the loop connecting strands β2 and β3. The opposite N terminus forms a shallow solvent-accessible pocket that is lined with hydrophobic residues in its center and with charged residues along its rim (SI Fig. 9). This pocket is a most likely candidate for the site of physical interaction with FecR, because a series of suppressor mutations in the signaling domain of FecA that have been shown to restore the ferric citrate-mediated transcriptional response to inactive FecR mutants (5, 14) is located in this pocket (SI Fig. 9).

Conserved Signal Transduction Network. How can we define those residues that contribute to the transmembrane signaling mechanism of FecA that couples ferric citrate binding at the cell surface to TonB recruitment in the periplasm? The difficulty in "seeing" an allosteric signaling mechanism, even with the structure of FecA in multiple states, highlights the need to develop novel approaches to answer these types of questions. One approach is statistical coupling analysis (SCA), a sequence-based method for identifying evolutionary interactions between residues in multiple sequence alignments (15). The premise of SCA is that conserved functional interactions between residues, regardless of mechanism or structural location, should drive their mutual evolution. Indeed, previous studies have shown that clusters of coevolving residues of protein families display two general properties: (*i*) they comprise a small fraction of the total number of residues, and (*ii*) they are organized into physically connected networks in the tertiary structure that link distant functional sites (15–17). Experimental studies show that these networks are involved in the long-range communication pathways of several well studied systems (15–17). Most recently, the evolutionary information extracted by SCA was sufficient to engineer *de novo* artificial members of a family of small-protein interaction modules (18, 19). These results demonstrate that, to a significant extent, SCA provides an accurate global picture of amino acid interactions in proteins.

We conducted SCA on multiple sequence alignments of 541 TonB-dependent transporters (barrel and plug) and 296 signaling domains (SI Figs. 10 and 11). Consistent with previous work, these analyses revealed a remarkably simple organization of evolutionary information for this protein family. A single primary cluster of coevolving residues was identified for the barrel and plug and for the signaling domain. Other positions within the multiple sequence alignments either were not conserved or display weaker coevolutionary signals despite having moderate degrees of sequence conservation.

The spatial organization of the coevolving residues found in the barrel and plug and the signaling domain provides a rational hypothesis for the ferric citrate-mediated signal transduction network of FecA (Fig. 3). In the barrel and plug, coevolving residues form a contiguous network of van der Waals interactions that begin at the cell surface at the base of the seventh and eighth extracellular loops of the barrel, running adjacent to the ferric citrate binding site along the interface between the barrel and the plug, and ending in the periplasmic pocket near the switch helix and the TonB-box (Fig. 3*A*). In addition, a branch of this network bifurcates to extend across the periplasmic

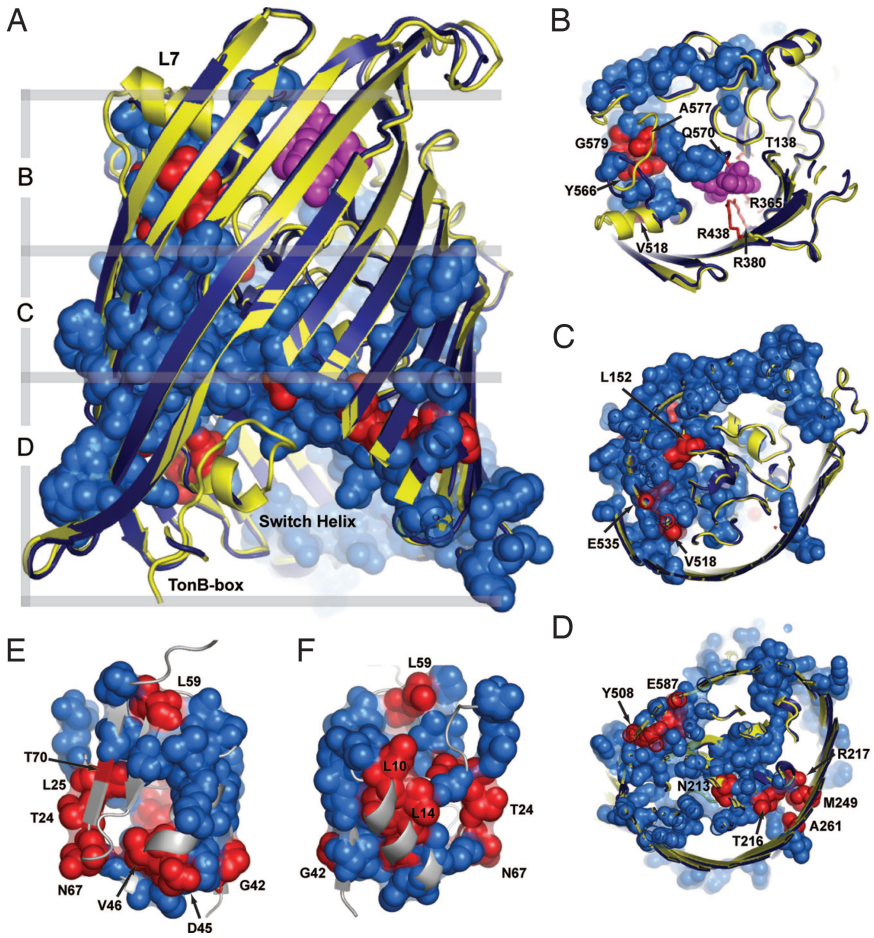

Fig. 3. Coevolving networks of the barrel and plug and the signaling domain link distant functional sites within FecA. (*A*) Ribbon diagrams of the unliganded (yellow) and liganded (blue) conformations of FecA. Residues T138, R365, R380, R438, and Q570 form the ferric citrate binding site (red sticks) and are each located within 3.5 Å of the ferric citrate molecule (magenta CPK model). The SCA-derived network of the barrel and plug has been mapped onto the structure with the van der Waals surfaces associated with these residues colored blue. The locations of those point mutations described in Table 1 are shown in red. (*B–D*) Serial sections through FecA as viewed from the solvent. (*E* and *F*) Ribbon diagrams of the signaling domain of FecA (silver). The SCA-derived network of the signaling domain has been mapped onto the structure with the van der Waals surfaces associated with these residues colored blue. The locations of those point mutations described in Table 1 are shown in red.

surface of the plug to terminate in the barrel wall across from the switch helix. This physical connectivity is significant given that only a small fraction of residues (≈17%) form most of the network and that no structural information was used to identify these positions. In summary, the residues identified link the extracellular and periplasmic pockets of FecA, which undergo ferric citrate-mediated conformational changes through a specific network of packing interactions. In addition, the network predicts a functional role for additional sites on the periplasmic surface of FecA that were not revealed by crystallographic studies.

In the signaling domain, the coevolving network extends from the top of the domain along the inward-facing surfaces of helices α1 and α2 and culminates at the proposed site of interaction with FecR (Fig. 3 *E* and *F* and SI Fig. 9). The precise orientation of the signaling domain with respect to the barrel and plug, and any potential change in its relative position or conformation after ferric citrate binding remain undefined. Nevertheless, it is clear that the TonB-box is likely to physically and functionally link the coevolving network of the barrel and plug to that of the signaling domain.

Evaluating the Signal Transduction Network. Directed mutagenesis of residues located throughout the barrel and plug and the signaling domain was used to assess whether these coevolving residues were indeed part of the ferric citrate-mediated signal transduction network of FecA (Fig. 3 and Table 1). We used a whole-cell GFP reporter assay (5, 20), in which GFP expression is under the control of the *fecA* promoter and is regulated by ferric citrate binding to FecA. This transcriptional assay measures the final output of all information flow steps in the ferric citrate-mediated signaling process and therefore should provide a quantitative physiologic assessment of the TonB-dependent allosteric communication pathway of FecA. For example, mutating those residues in FecA that directly contact the ferric citrate molecule (T138, R365, R380, R438, and Q570) or by removing the seventh (Δ519–533) or eighth (Δ563–577) extracellular loops of the barrel abrogates the transcriptional response to ferric citrate binding (Table 1) (20). These findings demonstrate the utility of this assay in judging the functional effects of our directed mutagenesis.

Using this assay we evaluated the functional effects of mutating coevolving residues of the barrel and plug (Table 1). Residues L152 from the plug, A261 from strand β3, Y508 and T517 from strand β13, E535 from strand β14, Y566 from the eighth extracellular loop, or G579 from strand β16 are positioned along the interface between the plug and the interior barrel wall. Mutating any one of these coevolving residues or the nearly fully

Table 1. Transcriptional activation by FecA mutants

Mutation	Position	Fluorescence
FecIR	—	0
FecIRA	—	1
L10A	Signaling, α1	0.71
A13G	Signaling, α1	1.24
L14A	Signaling, α1	0.95
Y17A	Signaling, α1	0.85
T24A	Signaling, β2	1.06
L25A	Signaling, β2	0.92
G42A	Signaling, β3	0
D43A	Signaling, β3	1.09
D45A	Signaling, L5	0
V46A	Signaling, α3	1.13
L59A	Signaling,β4	0
N67A	Signaling, L7	1.13
T70A	Signaling, β5	0.06
Δ28–30	Signaling, α2	0
Δ80–86	TonB-box	0
T138A	Binding site	0.15
R365A	Binding site	0
R380A	Binding site	0
R438A	Binding site	0
Q570A	Binding site	0
L152A	Plug	0.46
N213A	Plug	1.35
T216A	Plug	1
R217A	Plug	1.14
M249A	Barrel, β2	1.29
A261G	Barrel, β3	0.08
Y508A	Barrel, β13	0
T517A	Barrel, β13	0.18
V518A	Barrel, L7	0.80
E535A	Barrel, β14	0
E541A	Barrel, β14	0.87
R545A	Barrel, β14	0.96
N564A	Barrel, β15	1.26
Y566A	Barrel, L8	0
A577G	Barrel, L9	1.02
G579A	Barrel, β16	0
E587A	Barrel, β16	0
Δ519–533	Barrel, L7	0
Δ568–577	Barrel, L8	0

Coevolving residues identified by SCA are shown in bold. Induction of *fecA* transcription was measured by using *E. coli* strain AA93 harboring plasmid pLCIRA (FecIRA) and the GFP reporter plasmid pGFPA′ or plasmids pMM0203 (FecIR) and pGFPA′ (5, 20). The reported fluorescence values are the average of two independent experiments conducted in triplicate and represent the normalized relative fluorescence intensities of FecA mutants compared with that of wild-type FecA. We define the wild-type FecA transcriptional response to be 1 ± 0.2 based on the finding that the average experimental error in measured values for many trials of wild-type FecA is 20%. SDS/PAGE gels and Western blots were used to demonstrate that all FecA mutants are expressed and correctly targeted to the outer membrane (data not shown). Previous studies report slightly different transcriptional activation values for some mutants (14, 20). However, our data are in qualitative agreement with this study, which utilized a LacZ reporter assay instead of the whole-cell GFP reporter assay presented here.

conserved residue E587 from strand β16 severely disrupts signal transmission across the outer membrane and transcriptional activation in the cytoplasm. In total, mutating 11 of 16 coevolving residues located throughout the barrel and plug decreased or abrogated the transcriptional response (Table 1). This is a significant result given that none of the mutated residues are part of the ferric citrate binding site or the TonB-box; rather, these residues comprise a range of positions along the network linking the two. These results support the premise that the coevolving network of the barrel and plug forms to the ferric citrate-mediated signal transduction pathway of FecA within the outer membrane.

It is important to note that SCA did not identify those residues that form the ferric citrate binding site (Fig. 3*B*). This result makes sense; the SCA identifies conserved, rather than idiosyncratic, functional properties of proteins. For example, given the exceptional specificity that TonB-dependent transporters display for one or a highly restricted group of siderophores, those residues that coordinate siderophore binding are not expected to be conserved regardless of their apparent functional importance for a particular transporter. Indeed, these positions are nearly completely unconserved in the multiple sequence alignment (SI Fig. 12). However, despite considerable variations in siderophore specificity, conformational changes in the extracellular and periplasmic pockets are conserved among other TonB-dependent transporters (2, 3, 21). Collectively, these findings suggest that the fundamental design principle of TonB-dependent transporters is to conserve the underlying central transmembrane signaling mechanism that is used to propagate the signal indicating transporter occupancy across the outer membrane, while retaining the capacity for idiosyncratic variation in the siderophore binding site to accommodate the diverse chemical space of siderophores.

The ferric citrate-mediated signal transduction pathway of FecA can also be disrupted by directed mutagenesis of residues within the signaling domain (Table 1). $^{1}H/^{15}N$-HSQC spectra collected for signaling domain mutants D45A and T70A show that they are properly folded (SI Fig. 13). However, perturbations at these locations abrogated the transcriptional response to ferric citrate binding at the cell surface. Residue D45 is part of the proposed FecR binding pocket (SI Fig. 9). Mutating this position may inhibit the interaction between the signaling domain and FecR and thereby signal transmission across the cytoplasmic membrane. Mutating residue T70, which is found on the solvent-exposed surface of strand β5, unexpectedly abolished the transcriptional response. Additional signaling domain mutants G42A, L59A, and Δ28–30 are misfolded (SI Fig. 13) and are incapable of signal transmission (Table 1). Residues G42, D45, and L59 are part of the coevolving network of the signaling domain that functionally link residues found near the TonB-box to those residues of the FecR binding site (Fig. 3*E* and SI Fig. 9).

We also confirm that transcriptional activation of the ferric citrate import operon requires the TonB-box (20). Directed mutagenesis of the TonB-box or its removal abolishes signaling activity (Table 1), underscoring the essential role of this region in the signal transduction pathway of FecA. Comparing the chemical shift dispersion of the $^{1}H/^{15}N$-HSQC spectra for the signaling domain of FecA in the absence and presence of ferric citrate or the periplasmic domain of TonB (residues 154–239) demonstrates that the majority of the backbone amide resonances are unchanged (22). These results indicate that, when separated from the barrel and plug, the signaling domain of FecA does not interact with ferric citrate or TonB. We conclude that the TonB-box is required to establish the functional connectivity between the coevolving network of the barrel and plug to that of the signaling domain.

Discussion

The TonB-dependent transporters provide a well defined model system for addressing a fundamental problem in structural biology: understanding information flow between distant sites in proteins. These proteins couple the free energy change induced by siderophore binding at the cell surface with long-range conformational changes at the periplasmic surface. Despite considerable prior structural and biochemical work, the structural basis for this allosteric communication has remained largely

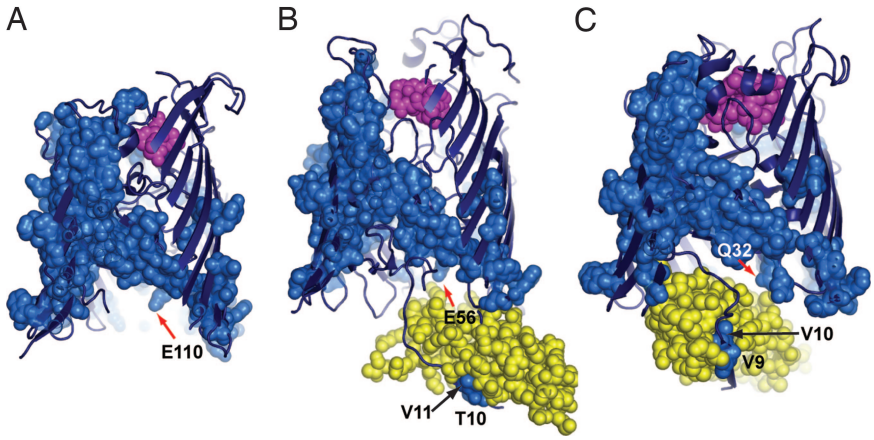

Fig. 4. Conserved signal transduction network for TonB-dependent transporters. Shown are ribbon diagrams of the liganded conformations of FecA (*A*), and FhuA (*B*) and BtuB (*C*) in complex with the periplasmic domain of TonB (yellow CPK model). The SCA-derived network has been mapped onto these structures with the van der Waals surfaces associated with these residues colored blue. The ferric citrate (FecA), ferrichrome (FhuA), and vitamin B_{12} (BtuB) molecules are shown as magenta CPK models.

unexplained. The evolutionary analysis and experimental data presented here provide a specific model: an ancient highly conserved mechanism underlies the siderophore-mediated signal transduction pathway of TonB-dependent transporters. The mechanism involves a sparse but connected network of residues that extend from the extracellular pocket of the barrel, running adjacent to the ferric citrate binding site along the interface between the barrel and the plug and splitting into two branches at the periplasmic surface of the transporter. The fact that a relatively small number of residues comprise this pathway explains how TonB-dependent transporters can simultaneously maintain plasticity for facile evolution of siderophore binding specificity while stably retaining a complex transmembrane signaling mechanism that is central to its physiological role in iron acquisition.

An independent test of this model came with the recent determination of the structure of the periplasmic domain of TonB in complex with two TonB-dependent receptors, FhuA (23) and BtuB (24). The coevolving signaling network bifurcates near the periplasmic surface of the transporter, with the first branch ending in the pocket containing the switch helix and the TonB-box and the second extending across the periplasmic surface of the plug to the opposite side of the barrel (Fig. 4). Consistent with prior expectations, these structures illustrate that the unwinding of the switch helix (one component of the siderophore-mediated conformational change in the transporter) causes the N terminus of TonB-dependent transporters to adopt an extended dynamic configuration. This conformational change facilitates the interaction between the TonB-box of the transporter and the periplasmic domain of TonB by interprotein β-strand exchange (23, 24). In either the FhuA-TonB or BtuB-TonB complexes, coevolving residues within the TonB-box that are disordered in the absence of TonB are revealed to comprise part of the new β-strand that forms direct interactions with TonB. These structures also show that the branch of the coevolving network that extends across the surface of the plug and into the barrel (encompassing several loops of the plug and the periplasmic base of β-strands 17, 20, 21, and 22) comprises a second surface for direct interaction with TonB. Interestingly, although FhuA and BtuB display overlapping but distinct binding sites for TonB, both binding modes support direct interactions with the sparse network of coevolving residues. For example, one specific polar interaction (E110 in FecA) that has been deemed to be important in binding TonB in both complexes is identified as part of the SCA-derived network (Fig. 4*A*). Collectively, these findings strongly support the model that the network of mutually evolving residues contributes to a conserved mechanism of allosteric communication in the diverse family of TonB-dependent transporters.

Materials and Methods

Strains and Plasmids. The *fecA* and *pupA* coding regions were PCR-amplified from *Escherichia coli* and *P. putida* genomic DNA. PCR products were digested with BamHI and XhoI and ligated into pGEX4T3. Directed mutagenesis of *fecA* within pLCIRA (5, 20) was carried out by using the QuikChange site-directed mutagenesis kit. *E. coli* strain AA93 (9) was transformed with the above constructs. All constructs were verified by DNA sequencing, and primer sequences are available upon request.

Protein Expression and Purification. The signaling domains of FecA and PupA were expressed in *E. coli* BL21(DE3) cells. For protein expression, cells grown to an OD_{600} of 0.6 were induced with 0.4 mM IPTG for 16 h at 30°C. Cells were harvested by centrifugation, resuspended in lysis buffer (50 mM Tris, pH 8.0/150 mM NaCl/0.1% Triton X-100/10 mg/liter lysozyme/5 mg/liter DNase I), and lysed by sonication. Cell lysates were centrifuged at $40{,}000 \times g$ for 30 min at 4°C. Fusion proteins were purified from cell lysates by absorption to glutathione agarose resin. The signaling domains were cleaved from the vector-encoded GST-tag with thrombin and were further purified by ion exchange and gel filtration chromatography.

NMR Spectroscopy. Uniformly ^{15}N- or ^{15}N, ^{13}C-labeled proteins were produced by supplementing M9 media with 1 g/liter ^{15}N-ammonium chloride, 3 g/liter ^{13}C-D-glucose, 0.5 ml/liter 0.5% thiamine, 2 mM $MgSO_4$, 0.1 mM $CaCl_2$, 0.5 ml/liter biotin (10 mg/ml), and 100 μg/ml carbencillin. All NMR experiments were acquired at 25°C with Varian INOVA spectrometers operating at proton frequencies of 500 and 600 MHz by using 1 mM protein samples dissolved in 50 mM NaPi (pH 6.0) and 50 mM NaCl. NMR data were processed with NMRPipe (25) and analyzed with SMARTNOTEBOOK (26) and NMRView (27). Backbone and aliphatic side chain chemical shift assignments were obtained from standard triple-resonance experiments. Aromatic side chain chemical shifts were assigned with 2D DQF-COSY and 2D NOESY (τ_m = 120 ms) experiments by using ^{15}N-labeled protein samples in 99.9% D_2O. Stereospecific chemical shift assignments for valine and leucine methyl groups were

obtained with two constant-time $^{1}H/^{13}C$-HSQC experiments (28- and 43-ms delay) by using 10% ^{13}C-labeled samples (28). Residual dipolar couplings were extracted from in-phase antiphase experiments by using ^{15}N-labeled samples aligned in 5% polyacrylamide stretched gels (29). Distance restraints were obtained from 3D ^{15}N-edited NOESY (τ_m = 150 ms) and ^{13}C-edited NOESY (τ_m = 100 ms) spectra recorded from ^{15}N- or ^{15}N, ^{13}C-labeled proteins. Restraints for the dihedral backbone angles were obtained from TALOS (30). Error bounds for these restraints were set to twice the standard deviation of the predictions with a minimum bound of ±30°. Coupling constants extracted from HNHA experiments provided additional dihedral angle constraints for structure calculations (31). Hydrogen bond constraints were established for those amide protons protected from D_2O exchange with $^{1}H/^{15}N$-HSQC experiments.

Structure calculations were performed with ARIA (32). ARIA runs were initiated by using a set of NOEs manually assigned from ^{15}N-edited NOESY spectra. NOEs from ^{13}C-edited spectra were introduced into the calculation once an initial ensemble of low-energy structures was obtained. MOLMOL (33) was used to assign carbonyl partners for amide protons that were protected from D_2O exchange. Hydrogen bond restraints were set to 1.3 Å $< d_{NH\text{-}O} <$ 2.5 Å and 2.3 Å $< d_{N\text{-}O} <$ 3.5 Å, respectively. Protein alignment tensors calculated with PALES (34) were used for structural refinement against residual dipolar coupling data.

SCA. SCA was conducted as previously described (15–19) on multiple sequence alignments comprised of 541 TonB-dependent transporters (barrel and plug) and 296 signaling domains. Sequences were collected by using PSI-BLAST (*e* scores <0.001) and automatically aligned by using Cn3D (35) and MUSCLE (36), followed by manual adjustment. Both alignments are available upon request. The coordinates for the signaling domains of FecA and PupA (NMR structures) and the crystallographic structures of FhuA (3), FepA (37), FecA (2), BtuB (21), FpvA (38), and FptA (39) were used to construct the alignments. For an alignment with n positions and m sequences, the SCA produces a symmetric $n \times n$ matrix of coupling scores. To identify the network of evolutionarily coupled residues, we used either hierarchical clustering (signaling domain) (16, 17, 40) or independent component analysis (ICA) (barrel/plug) to find the dominant cluster of sequence positions whose interaction best represents the information content of the SCA matrix. The ICA approach for analysis of the SCA data set is available upon request. ICA was carried out by using the MATLAB implementation of the Fast-ICA algorithm, available at www.cis.hut.fi/projects/ica/fastica.

GFP Fluorescence. To monitor *fecA* induction, *E. coli* strain AA93 harboring plasmids pLCIRA and pGFPA′ (5, 20) were grown in WL Nutrient Broth in the absence or presence of 1 mM sodium citrate at 37°C. The reported fluorescence values represent the normalized relative fluorescence intensities of FecA mutants compared with that of wild-type FecA.

We thank K. H. Gardner for providing computer resources; R. Martinez for participating in the initial phase of this work; W. P. Russ for assistance with data analysis; and V. Braun and A. Sauter (University of Tübingen, Tübingen, Germany) for plasmids, bacterial strains, and advice. J.D., R.R., and M.K.R. are investigators with the Howard Hughes Medical Institute. A.D.F. is a long-term fellow of the Human Frontier Science Program. This work was supported by a grant from the Welch Foundation (to J.D. and R.R.).

1. Ferguson AD, Deisenhofer J (2004) *Cell* 116:15–24.
2. Ferguson AD, Chakraborty R, Smith BS, Esser L, van der Helm D, Deisenhofer J (2002) *Science* 295:1715–1719.
3. Ferguson AD, Hofmann E, Coulton JW, Diederichs K, Welte W (1998) *Science* 282:2215–2220.
4. Enz S, Mahren S, Stroeher UH, Braun V (2000) *J Bacteriol* 182:637–646.
5. Enz S, Brand H, Orellana C, Mahren S, Braun V (2003) *J Bacteriol* 185:3745–3752.
6. Braun V, Mahren S, Sauter A (2005) *Biometals* 18:507–517.
7. Welz D, Braun V (1998) *J Bacteriol* 180:2387–2394.
8. Mahren S, Enz S, Braun V (2002) *J Bacteriol* 184:3704–3711.
9. Ochs M, Veitinger S, Kim I, Welz D, Angerer A, Braun V (1995) *Mol Microbiol* 15:119–132.
10. Angerer A, Enz S, Ochs M, Braun V (1995) *Mol Microbiol* 18:163–174.
11. Kim I, Stiefel A, Plantor S, Angerer A, Braun V (1997) *Mol Microbiol* 23:333–344.
12. Harle C, Kim I, Angerer A, Braun V (1995) *EMBO J* 14:1430–1438.
13. Garcia-Herrero A, Vogel HJ (2005) *Mol Microbiol* 58:1226–1237.
14. Breidenstein E, Mahren S, Braun V (2006) *J Bacteriol* 188:6440–6442.
15. Lockless SW, Ranganathan R (1999) *Science* 286:295–299.
16. Shulman AI, Larson C, Mangelsdorf DJ, Ranganathan R (2004) *Cell* 116:417–429.
17. Suel GM, Lockless SW, Wall MA, Ranganathan R (2003) *Nat Struct Biol* 10:59–69.
18. Russ WP, Lowery DM, Mishra P, Yaffe MB, Ranganathan R (2005) *Nature* 437:579–583.
19. Socolich M, Lockless SW, Russ WP, Lee H, Gardner KH, Ranganathan R (2005) *Nature* 437:512–518.
20. Sauter A, Braun V (2004) *J Bacteriol* 186:5303–5310.
21. Chimento DP, Mohanty AK, Kadner RJ, Wiener MC (2003) *Nat Struct Biol* 10:394–401.
22. Peacock RS, Andrushchenko VV, Demcoe AR, Gehmlich M, Lu LS, Herrero AG, Vogel HJ (2006) *Biometals* 19:127–142.
23. Pawelek PD, Croteau N, Ng-Thow-Hing C, Khursigara CM, Moiseeva N, Allaire M, Coulton JW (2006) *Science* 312:1399–1402.
24. Shultis DD, Purdy MD, Banchs CN, Wiener MC (2006) *Science* 312:1396–1399.
25. Delaglio F, Grzesiek S, Vuister GW, Zhu G, Pfeifer J, Bax A (1995) *J Biomol NMR* 6:277–293.
26. Slupsky CM, Boyko RF, Booth VK, Sykes BD (2003) *J Biomol NMR* 27:313–321.
27. Johnson BA (2004) *Methods Mol Biol* 278:313–352.
28. Neri D, Szyperski T, Otting G, Senn H, Wuthrich K (1989) *Biochemistry* 28:7510–7516.
29. Chou JJ, Gaemers S, Howder B, Louis JM, Bax A (2001) *J Biomol NMR* 21:377–382.
30. Cornilescu G, Delaglio F, Bax A (1999) *J Biomol NMR* 13:289–302.
31. Vuister GW, Bax A (1993) *J Am Chem Soc* 115:7772–7777.
32. Linge JP, O'Donoghue, Nilges M (2001) *Methods Enzymol* 339:71–90.
33. Koradi R, Billeter M, Wuthrich K (1996) *J Mol Graphics* 14:51–55.
34. Zweckstetter M, Bax A (2000) *J Am Chem Soc* 122:3791–3792.
35. Hogue CW (1997) *Trends Biochem Sci* 22:314–316.
36. Edgar RC (2004) *Nucleic Acids Res* 32:1792–1797.
37. Buchanan SK, Smith BS, Venkatramani L, Xia D, Esser L, Palnitkar M, Chakraborty R, van der Helm D, Deisenhofer J (1999) *Nat Struct Biol* 6:56–63.
38. Cobessi D, Celia H, Folschweiller N, Schalk IJ, Abdallah MA, Pattus F (2005) *J Mol Biol* 347:121–134.
39. Cobessi D, Celia H, Pattus F (2005) *J Mol Biol* 352:893–904.
40. Hatley ME, Lockless SW, Gibson SK, Gilman AG, Ranganathan R (2003) *Proc Natl Acad Sci USA* 100:14445–14450.
41. DeLano W (2002) PyMOL (DeLano Scientific, San Carlos, CA).